Energy Conversion and Management 123 (2016) 535–548

Contents lists available at ScienceDirect

Energy Conversion and Management

journal homepage: www.elsevier.com/locate/enconman

Parameters extraction of the three diode model for the multi-crystalline solar cell/module using Moth-Flame Optimization Algorithm

Dalia Allam, D.A. Yousri *, M.B. Eteiba

Department of Electrical Engineering, Faculty of Engineering, Fayoum University, Fayoum, Egypt

ARTICLE INFO

Article history:
Received 11 April 2016
Received in revised form 8 June 2016
Accepted 18 June 2016
Available online 6 July 2016

Keywords:
Double diode model
Flower Pollination algorithm
Hybrid Evolutionary technique
Modified double diode model
Moth-Flame optimizer
Parameters estimation
Three diode model

ABSTRACT

As a result of the wide prevalence of using the multi-crystalline silicon solar cells, an accurate mathematical model for these cells has become an important issue. Therefore, a three diode model is proposed as a more precise model to meet the relatively complicated physical behavior of the multi-crystalline silicon solar cells. The performance of this model is compared to the performance of both the double diode and the modified double diode models of the same cell/module. Therefore, there is a persistent need to keep searching for a more accurate optimization algorithm to estimate the more complicated models' parameters. Hence, a proper optimization algorithm which is called Moth-Flame Optimizer (MFO), is proposed as a new optimization algorithm for the parameter extraction process of the three tested models based on data measured at laboratory and other data reported at previous literature. To verify the performance of the suggested technique, its results are compared with the results of the most recent and powerful techniques in the literature such as Hybrid Evolutionary (DEIM) and Flower Pollination (FPA) algorithms. Furthermore, evaluation analysis is performed for the three algorithms of the selected models at different environmental conditions. The results show that, MFO algorithm achieves the least Root Mean Square Error (RMSE), Mean Bias Error (MBE), Absolute Error at the Maximum Power Point (AEMPP) and best Coefficient of Determination. In addition, MFO is reaching to the optimal solution with the shortest execution time when it is compared with the other tested algorithms.

1. Introduction

There are different types of the renewable energy resources, solar energy is the most important one due to its wide availability and its cleanliness. Solar energy is considered as an alternative solution to overcome the lack of the fossil fuels [1]. Therefore, the production of the photovoltaic cells has increased. Multi-crystalline solar cells in particular are widely used due to their low fabrication cost compared with the other types [2,3]. They are fabricated from a multi-crystalline silicon wafer which consists of single crystalline grains separated by grain boundaries with different crystallographic orientations [4,5]. The Losses in these cells are related to these grain boundaries, where the recombination is likely to take place [2,3,6–9]. Thus, introducing an accurate model which take into consideration the effect of the grain boundaries is a very essential target [10–12].

Generally, there are several mathematical models of PV solar cells that are starting from the simplest one which is the single diode model (SDM) and passing to the elaborated model such as the double diode model (DDM) until reaching to the more detailed models such as modified double diode (MDDM) and three diode (TDM). Utilizing more detailed models is an important aspect to deal with increasing the number of large PV installations especially at low irradiance conditions [13]. Furthermore, these detailed models are efficient in describing the physical behavior of the multi-crystalline silicon solar cells, because the effect of the grain boundaries, the carrier recombination and the leakage current are taken into account [10–14].

During the last decades, several optimization techniques for parameters identification of solar cell models have been proposed. These techniques can be classified into two categories; conventional and meta-heuristic algorithms. Some of the conventional techniques are presented in [15–17] for double diode model, for modified double diode model [12] and for three diode model [11]. However, these algorithms are time consuming and lose their ability to provide accurate solutions especially with the increased number of the estimated parameters [18]. Therefore, meta-heuristic algorithms are the alternative solution to overcome the problems of the conventional algorithms. The newest literature of the meta-heuristic algorithms for the parameters estimation process is as follows: In [19] Bacterial Foraging (BF) algorithm is

* Corresponding author.
E-mail address: day01@fayoum.edu.eg (D.A. Yousri).

http://dx.doi.org/10.1016/j.enconman.2016.06.052
0196-8904/

applied under normal and shading condition. Generalized Oppositional Teaching Learning Based Optimization (GOTLBO) [20] is developed to accelerate the speed of conversion for the optimal solution. A Differential Evolution with Integrated Mutation per iteration (DEAM) [21] and Hybrid Evolutionary algorithm (DEIM) [22] have exhibited a good performance in terms of accuracy and CPU-execution time. Flower Pollination algorithm [1] has shown unnoticed deviation between the experimental and the estimated (I-V) curves specially at low solar irradiance levels. Furthermore, Mutative-scale Parallel Chaos Optimization algorithm (MPCOA) [23], Artificial Bee Colony algorithm (ABC) [24], Artificial Bee Swarm Optimization algorithm (ABSO) [25], Harmony Search-based algorithm (HS) [26] Simulated Annealing algorithm (SA) [27] and Pattern Search technique [28] are proposed to extract the parameters of SDM and DDM based on an experimental data presented in [29]. Genetic algorithm [30] is applied to extract the global optimal parameters for SDM and DDM. Moreover, in [31], Bird Mating technique (BM) is used to estimate the SDM parameters for PV solar array.

From the previous literature, it's observed that several recent researches are using the most common models such as SDM and DDM. The more complicated models such as MDDM and TDM are seldom used in the recent investigations to avoid estimating larger number of parameters. However, it has been proven in this study that these models are more efficient in dealing with the more complicated physical behavior of the multi-crystalline solar cell/module. Also, the researches which study the MDDM [12] and TDM [11] relied on conventional algorithms. This resulted in less accurate results in parameters extraction process and they consume a longer time. Therefore, a more efficient algorithm should be introduced to estimate the parameters of these complicated models with more accuracy and with minimum execution time.

In this paper, more complicated models such as MDDM and TDM beside DDM are investigated based on two sources of data. The first one is the experimental data reported at previous literature for multi-crystalline solar cell under different levels of irradiance [12]. The other one is an experimental data measured at the laboratory for multi-crystalline solar module under different levels of temperature and irradiance. A newest optimization algorithm which is called Moth-Flame Optimizer (MFO) is proposed to extract the required parameters of the three suggested models. MFO algorithm inspired from the navigation method of moths in nature called transverse orientation [32]. The performance of the introduced algorithm is compared to the recent and efficient algorithms in the literature such as DEIM [22] and FPA algorithms [1]. To assess its validation, an evaluation analysis which include root mean square error, mean bias error, absolute error at the maximum power point and coefficient of determination, is performed. The results demonstrate that FPA technique is resulted in fair accurate results with short execution time. The accuracy of DEIM algorithm was found to be also fair however the execution time was found to be three times that of the FPA algorithm. While, the MFO algorithm proved to be the most efficient optimization algorithm for the models' parameters estimation with both the accuracy and the execution time compared to the other mentioned algorithms. Therefore, it is adapted in this investigation. Consequently, this accurate modeling gives a better performance of the whole solar system design which is reflected on the cost reduction.

The rest of this manuscript is organized as follows: 2nd section will discuss Photovoltaic (PV) models. The 3rd section illustrates the problem formulation. In Section 4, the Moth-Flame optimizer (MFO) is presented in details. The 5th section will show the evaluation analysis, simulation and the results will be discussed in Sections 6 and 7 contains the outcome of the paper.

2. Photovoltaic modeling

There are several mathematical models that describe the operation and the physical behavior of the photovoltaic generator. The need of more detailed models are becoming essential to meet the physical requirements of the multi-crystalline solar cell and module such as the effect of grain boundaries and the leakage current [10–12]. Therefore, the MDDM and the TDM models are studied as well as the DDM.

2.1. Double Diode Model (DDM)

The DDM is represented by a light generated current source in parallel with two diodes and a shunt resistance in addition to a series resistance as shown in Fig. 1. The current of the first diode I_{D1}

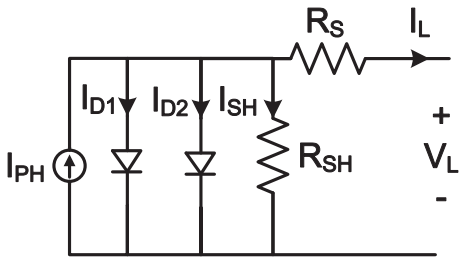

Fig. 1. Double diode model.

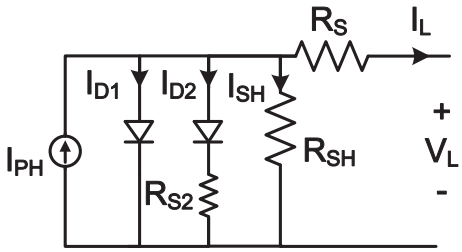

Fig. 2. Modified double diode model.

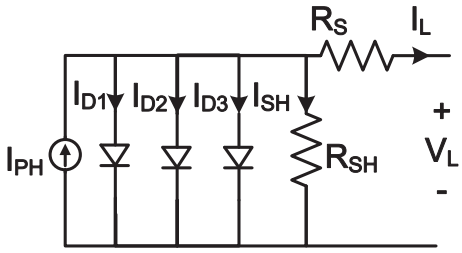

Fig. 3. Three diode model.

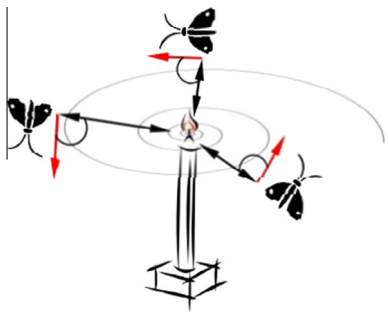

Fig. 4. Spiral flying path around close light sources [32].

represents the current due to diffusion and recombination in the Quasi Neutral Regions (QNRs) of the emitter and bulk regions of the P-N junction. The second diode current I_{D2} represents the current due to recombination in the Space Charge Regions (SCRs) [10,33,34]. The leakage current is accounted by the shunt resistance R_{SH}. Moreover, the material resistivity and the ohmic losses of the contacts are represented by a series resistance R_S [1]. Hence, the output current is calculated as follows:

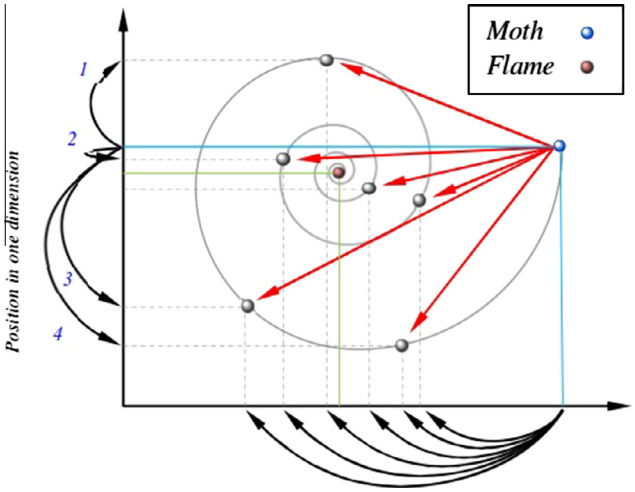

Fig. 5. Some of the possible positions that can be reached by a moth with respect to a flame using the logarithmic spiral [32].

$$I_L = I_{PH} - I_{D1} - I_{D2} - I_{SH} \tag{1}$$

$$I_L = I_{PH} - I_{O1}\left[\exp\left(\frac{q(V_L + I_L R_S)}{a_1 kT}\right) - 1\right] - I_{O2}\left[\exp\left(\frac{q(V_L + I_L R_S)}{a_2 kT}\right) - 1\right] - \frac{(V_L + I_L R_S)}{R_{SH}} \tag{2}$$

where I_L is the solar cell output current, I_{PH} is the light generated current, I_{SH} is the shunt current. I_{O1}, I_{O2} are the diffusion and the saturation currents. a_1, a_2 are the ideality factors of diode 1 and diode 2 respectively. R_S and R_{SH} are the series and the shunt resistances respectively. k is Boltzmanns constant. q is the electronic charge and T is the cell absolute temperature in Kelvin. From Eq. (2), seven unknown parameters (R_S, R_{SH}, I_{O1}, I_{O2}, a_1, a_2, I_{PH}) should be extracted for representing the real behavior of the solar cells. This estimation process can be done with the aid of an optimization technique.

2.2. Modified Double Diode Model (MDDM)

In the model of Fig. 2, an additional resistance R_{S2} is added in series with the second diode to take into account the effect of grain boundary region, since the resistivity in the vicinity of grain boundaries is higher than that within the crystallites [12].

The output solar cell current is calculated through the following Eq. (3):

$$I_L = I_{PH} - I_{O1}\left[\exp\left(\frac{q(V_L + I_L R_S)}{a_1 kT}\right) - 1\right] - I_{O2}\left[\exp\left(\frac{q(V_L + I_L R_S - I_{D2} R_{S2})}{a_2 kT}\right) - 1\right] - \frac{(V_L + I_L R_S)}{R_{SH}} \tag{3}$$

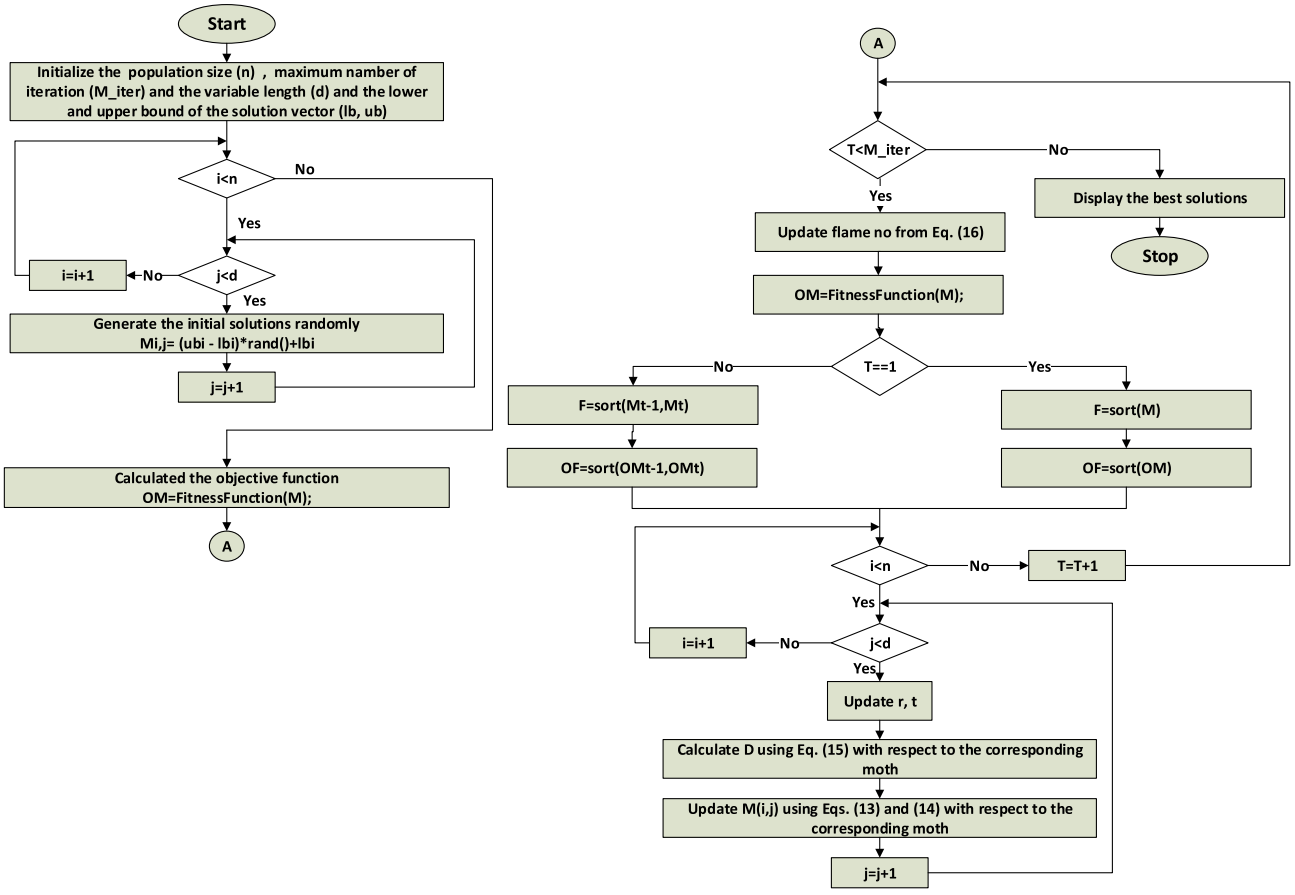

Fig. 6. Flow chart of Moth-Flame Optimization Algorithm.

There are eight unknown parameters at Eq. (3) (R_S, R_{S2}, R_{SH}, I_{O1}, I_{O2}, a_1, a_2, I_{PH}) are required to be estimated by the help of an optimization method.

2.3. Three Diode Model (TDM)

In this model, the influence of grain boundaries and large leakage current are taken into consideration [11]. Therefore, a third diode is added in parallel with the two diodes of the DDM as shown in Fig. 3.

By applying KCL, the output current is calculated as follows:

$$I_L = I_{PH} - I_{D1} - I_{D2} - I_{D3} - I_{SH} \tag{4}$$

$$I_L = I_{PH} - I_{O1}\left[\exp\left(\frac{q(V_L + I_L R_S)}{a_1 kT}\right) - 1\right] - I_{O2}\left[\exp\left(\frac{q(V_L + I_L R_S)}{a_2 kT}\right) - 1\right] - I_{O3}\left[\exp\left(\frac{q(V_L + I_L R_S)}{a_3 kT}\right) - 1\right] - \frac{(V_L + I_L R_S)}{R_{SH}} \tag{5}$$

where I_{D1} is the diffusion current with $a_1 = 1$, I_{D2} is the recombination current with $a_2 = 2$. Also, I_{D3} represents the current due to recombination in the defect regions, grain boundaries, etc. with $a_3 > 2$ depending on [9,35,36]. The other terms are reported

Table 1
The extracted parameters for DDM. MDDM and TDM for Q6-1380 solar cell by MFO and DEIM, FPA techniques at different irradiance and room temperature.

Irradiance levels		Parameters									
		R_S(Ω)	R_{S2} (Ω)	R_{SH} (Ω)	I_{O1} (μA)	a_1	I_{O2} (mA)	a_2	I_{O3} (mA)	a_3	I_{PV} (A)
At 20 mW/cm^2	*DDM*										
	MFO	0.439	–	1100	1	2.500	0.3178	3.768	–	–	0.0396
	DEIM	0.4320	–	1100	0.0467	2.2954	0.3125	3.7301	–	–	0.0396
	FPA	0.6145	–	881.71	0.67430	1.9379	0.3552	4.0041	–	–	0.0396
	MDDM										
	MFO	0.1840	1.5682	590	0.13663	1.6938	0.2076	3.1668	–	–	0.03951
	DEIM	0.1605	1.6794	499.5830	0.72217	1.9626	0.2058	3.1803	–	–	0.0394
	FPA	0.1716	1.2411	561.3792	0.67163	2.0174	0.2530	3.3560	–	–	0.03952
	TDM										
	MFO	0.8215	–	1001.9883	3.5685e−5	–	1.000e−06	–	0.2329	3.5625	0.03966
	DEIM	0.7902	–	1052.8485	3.5133e−5	–	1.000e−06	–	0.2456	3.5980	0.03967
	FPA	0.8581	–	1070.4920	2.5433e−5	–	1.0925e−04	–	0.2491	3.6117	0.03995
At 9.84 mW/cm^2	*DDM*										
	MFO	0.5721	–	1100	1	2.4999	0.2765	3.6211	–	–	0.01951
	DEIM	0.5163	–	1100	1.00e−6	2.2330	0.2816	3.6192	–	–	0.01951
	FPA	0.5578	–	730.4283	0.3763	2.4312	0.2705	3.6003	–	–	0.01950
	MDDM										
	MFO	0.17400	1.5227	590.3262	0.15251	1.7010	0.19980	3.1595	–	–	0.01944
	DEIM	0.13650	1.8683	590.34288	0.7660	1.98040	0.18877	3.1140	–	–	0.019447
	FPA	0.14608	1.3744	593.06025	0.766949	2.0244	0.238165	3.3384	–	–	0.01945
	Three diode										
	MFO	0.9900	–	1001.1048	8.4823e−5	–	1.000e−06	–	0.2287	3.4645	0.01954
	DEIM	0.8932	–	1025.1551	6.0824e−5	–	1.000e−06	–	0.2413	3.5021	0.01954
	FPA	0.7323	–	921.9762	1.000e−6	–	3.4782e−04	–	0.2479	3.5522	0.01950
At 3.47 mW/cm^2	*DDM*										
	MFO	0.1500	–	1100	1.000e−6	2.4999	0.3810	3.8878	–	–	0.00691
	DEIM	0.1473	–	1100	0.9398	2.4465	0.3365	3.7759	–	–	0.00688
	FPA	0.1795	–	1099.99	0.02203	2.500	0.2961	3.6368	–	–	0.00696
	MDDM										
	MFO	0.1050	1.7175	607.9995	0.43830	1.7856	0.1894	3.0976	–	–	0.00686
	DEIM	0.1069	1.9500	592.4947	0.49382	1.8194	0.19135	3.1106	–	–	0.00687
	FPA	0.15366	1.3752	582.9046	0.93991	2.0320	0.17510	3.10377	–	–	0.006868
	TDM										
	MFO	0.7146	–	1099.4564	1.5257e−4	–	1.000e−06	–	0.2818	3.5493	0.006910
	DEIM	0.5764	–	1100	9.1121e−5	–	1.000e−06	–	0.2970	3.6014	0.006913
	FPA	0.85728	–	1100	3.0937e−4	–	1.000e−03	–	0.3294	3.6886	0.006910
At 0.58 mW/cm^2	*DDM*										
	MFO	0.6455	–	1100	0.82510	2.2491	0.2941	3.6006	–	–	0.00120
	DEIM	0.6574	–	1100	0.5992	2.2133	0.2849	3.5685	–	–	0.00117
	FPA	0.8441	–	692.0026	0.8199	2.3147	0.2328	3.3772	–	–	0.001139
	MDDM										
	MFO	0.1010	1.7252	608.0038	0.20299	1.7872	0.177603	3.0682	–	–	0.001159
	DEIM	0.11854	1.9678	608.4871	0.75252	1.9920	0.16618	3.0145	–	–	0.001165
	FPA	0.13919	1.38192	654.5989	0.98150	2.1538	0.192277	3.1824	–	–	0.0011595
	TDM										
	MFO	1.04484	–	1100	2.4130e−4	–	1.000e−03	–	0.2522	3.3861	0.00120
	DEIM	1.0600	–	996.0804	1.12695e−4	–	0.73447	–	0.2668	3.4820	0.00119
	FPA	1.0562	–	1038.0407	2.7708e−4	–	1.1424e−03	–	0.2401	3.4071	0.00118

previously. At Eq. (5), only seven parameters (R_S, R_{SH}, I_{O1}, I_{O2}, I_{O3}, a_3, I_{PH}) are needed to be estimated.

3. Problem formulation

The main target of the solar cell modeling is minimizing the difference between the experimental data and the extracted ones under various environmental conditions by extracting the optimal values of the unknown parameters of the models.

The main requirements to apply any optimization algorithm are accomplished by the determination of the vector of solutions (X), the search range and the objective function [1].

The solution vectors are defined as follows; X = (R_S, R_{SH}, I_{O1}, I_{O2}, a_1, a_2, I_{PH}) for DDM, X = (R_S, R_{S2}, R_{SH}, I_{O1}, I_{O2}, a_1, a_2, I_{PH}) for MDDM. While X = (R_S, R_{SH}, I_{O1}, I_{O2}, I_{O3}, a_3, I_{PH}) for TDM, where $a_1 = 1$ and $a_2 = 2$.

According to the previous literature, the lower and the upper boundaries of the parameters are selected as follows; R_S, R_{S2} are with in the range[0 2], R_{SH} is $\in$ [100 5000], I_{O1}, I_{O2}, I_{O3} are $\in$ [0 $1e-12$], a_1, a_2, a_3 are $\in$ [1 5] and $I_{PH} \in [0\ 2I_{SH}]$, where I_{SH} is the short circuit current [18].

The objective function is defined as the RMSE. The error function ($J(V_L, I_L, X)$) is the difference between the estimated and the experimental currents. ($J(V_L, I_L, X)$) is expressed as follows in Eq. (6)

$$J(V_L, I_L, X) = I_L - I_{L-exp} \tag{6}$$

where the estimated current I_L can be calculated from Eqs. (2), (3) and (5) for DDM, MDDM and TDM models respectively. I_{L-exp} is the measured current.

The objective function is defined by Eq. (7)

$$RMSE = \sqrt{\frac{1}{K}\sum_{i=1}^{K} J(V_t, I_t, X)^2} \tag{7}$$

where K is the number of the readings of the measured data.

The proposed optimization techniques (MFO, DEIM, and FPA) are mainly used to extract the optimal parameters of the three models with minimum objective function (RMSE).

4. Analysis of Moth-Flame Optimization Algorithm

MFO is a new population-based algorithm developed by Mirjalili in November 2015 [32] and was inspired by the navigation method of moths in nature called transverse orientation.

4.1. Characteristics of moths

Moths are fancy insects, they have special navigation methods in night which is called transverse orientation. In this mechanism, they fly at night by maintaining a fixed angle with respect to the moon, this method very helpful for traveling in a straight line specially when the light source is very far. When the light source

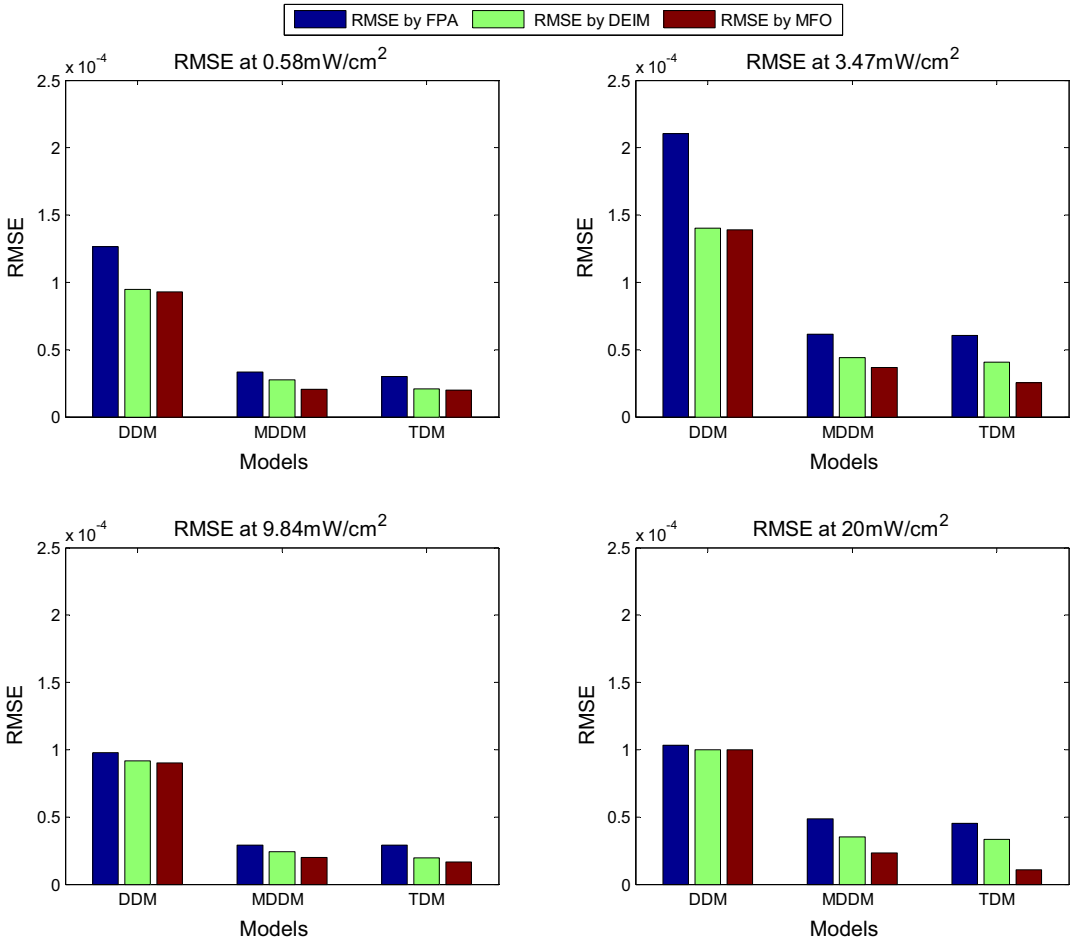

Fig. 7. RMSE for DDM, MDDM and TDM models of Q6-1380 solar cell by FPA, DEIM and MFO algorithms at different irradiance and room temperature.

is close, moths fly spirally around it and finally converge toward it after just a few corrections as illustrated from Fig. 4 [32].

4.2. MFO algorithm

The key components in the MFO algorithm are moths and flames where both of them are considered as a solution, however, they differ in the way of their treatment and their updating in each iteration. The moths are actual search agents that move around the search space, while flames are the best position of moths that obtained so far. Thus, flames can be considered as flags that are dropped by moths when searching the search space. Therefore, each moth searches around a flag and updates it in case of finding a better solution. With this method, a moth never lose its best solution [32].

Since the MFO algorithm is a population-based algorithm, the set of moths can be represented in a matrix as follows [32]:

$$M = \begin{pmatrix} m_{1,1} & m_{1,2} & m_{1,3} & \dots & m_{1,d} \\ m_{2,1} & m_{2,2} & m_{2,3} & \dots & m_{2,d} \\ \vdots & \vdots & \vdots & \ddots & \vdots \\ m_{n,1} & m_{n,2} & m_{n,3} & \dots & m_{n,d} \end{pmatrix} \tag{8}$$

For all the moths, there is an array for storing the corresponding objective function (fitness) values as follows [32]:

$$OM = \begin{pmatrix} OM_1 & OM_2 & \dots & OM_n \end{pmatrix}^T \tag{9}$$

where n is the number of the moths and d is the problem's variables. T is transpose.

Consequently, the flames can be represented also in a matrix similar to the moths matrix as follows [32]:

$$F = \begin{pmatrix} F_{1,1} & F_{1,2} & F_{1,3} & \dots & F_{1,d} \\ F_{2,1} & F_{2,2} & F_{2,3} & \dots & F_{2,d} \\ \vdots & \vdots & \vdots & \ddots & \vdots \\ F_{n,1} & F_{n,2} & F_{n,3} & \dots & F_{n,d} \end{pmatrix} \tag{10}$$

Also, there is an array for storing the corresponding fitness values as follows:

$$OF = \begin{pmatrix} OF_1 & OF_2 & \dots & OF_n \end{pmatrix}^T \tag{11}$$

The general structure of the MFO algorithm contains three-tuple approximation functions that are summarized as follows [32]:

$$\text{MFO} = (\text{I}, \text{P}, \text{T}).$$

I is the initialization function that creates a random population of moths and their corresponding fitness values as defined as follows [32].

$$\begin{aligned} M(i,j) &= (ub(i) - lb(i)) * rand() + lb(i). \\ OM &= FitnessFunction(M). \end{aligned} \tag{12}$$

where ub, lb are the upper and lower bounds of the variables respectively.

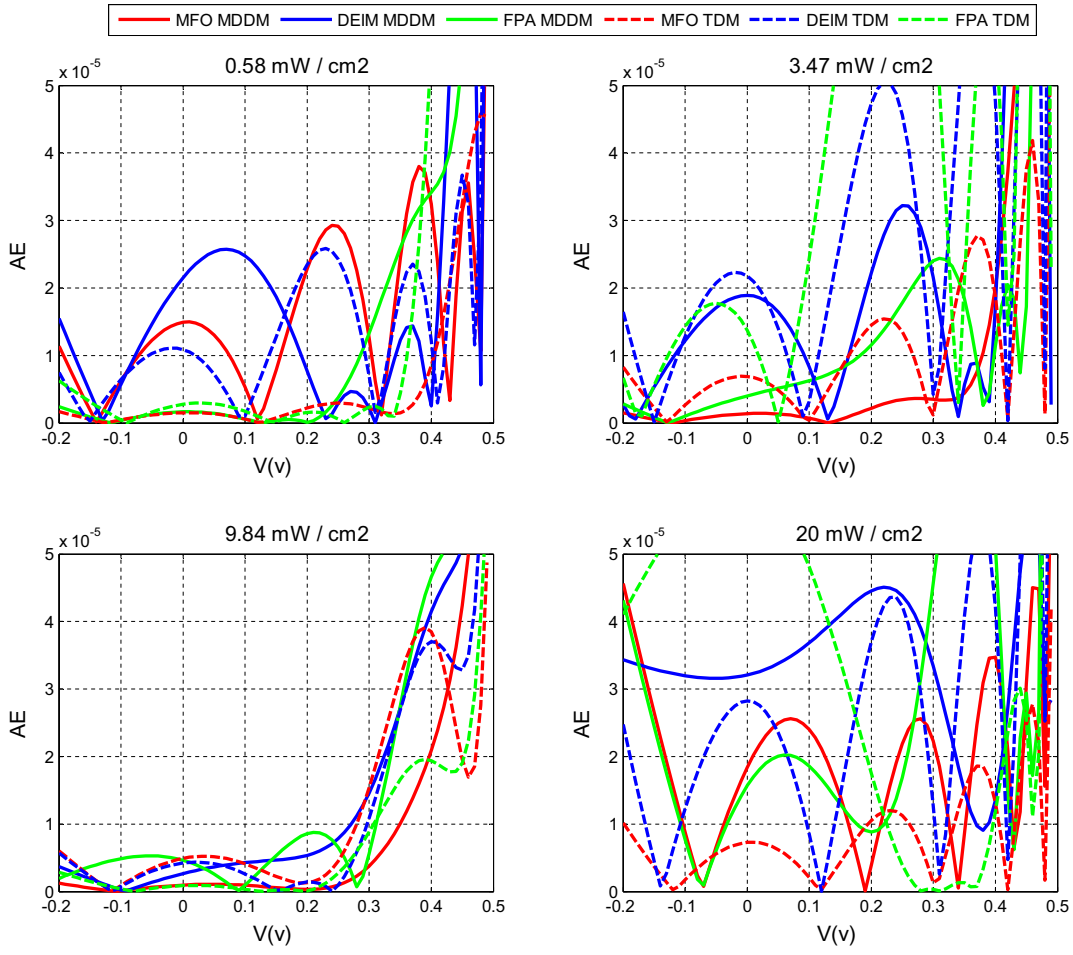

Fig. 8. Absolute error with respect to cell voltage for MDDM and TDM by different algorithms at different irradiance and room temperature.

Table 2
RMSE, MBE, AE at MPP and R^2 of various techniques for three models of Q6-1380 solar cell at different irradiance and room temperature.

	At 20 mW/cm^2			At 9.84 mW/cm^2			At 3.47 mW/cm^2			At 0.58 mW/cm^2		
	DDM	MDDM	TDM	DDM	MDDM	TDM	DDM	MDDM	TDM	DDM	MDDM	TDM
RMSE												
MFO	1.0005e−04	1.3419e−05	1.0867e−05	9.0172e−05	1.9904e−05	1.6762e−05	1.3895e−04	3.6712e−05	2.5542e−05	9.2898e−05	2.0648e−05	2.0144e−05
DEIM	1.0007e−04	3.5325e−05	3.3385e−05	9.1832e−05	2.4353e−05	1.9837e−05	1.4017e−04	4.4026e−05	4.0609e−05	9.4866e−05	2.7693e−05	2.0918e−05
FPA	1.0323e−04	4.8564e−05	4.5235e−05	9.7982e−05	3.0946e−05	2.9089e−05	2.1061e−04	6.1391e−05	6.0556e−05	1.2661e−04	3.3465e−05	3.0115e−05
MBE												
MFO	1.6349e−06	2.5587e−07	4.0150e−08	1.2522e−07	1.2353e−07	8.6329e−09	4.3320e−06	4.1097e−08	1.5494e−08	5.4539e−07	6.5237e−08	5.0113e−08
DEIM	5.6882e−06	5.5773e−06	1.7840e−07	1.3648e−05	1.8583e−07	1.0740e−07	6.3659e−07	6.7633e−06	2.4108e−07	3.9032e−06	3.0829e−06	1.2934e−06
FPA	5.7011e−06	3.6844e−05	1.6715e−05	5.5643e−06	3.1668e−06	3.1467e−06	9.2920e−05	1.01393e−05	1.0345e−05	2.6777e−05	1.6514e−05	1.4470e−05
AE at MPP												
MFO	1.2952e−05	5.7537e−06	3.9547e−06	1.6434e−05	7.8698e−06	1.6401e−05	3.9792e−05	5.3081e−06	4.7405e−06	7.0086e−06	7.6354e−07	7.5895e−07
DEIM	1.5154e−05	9.9903e−06	1.7488e−06	2.0422e−05	2.0053e−05	7.3028e−06	2.5032e−05	5.5531e−06	2.0458e−05	6.8953e−06	2.1674e−06	9.6032e−07
FPA	6.6361e−06	3.0053e−05	1.1724e−07	9.9741e−06	9.8748e−06	9.027e−06	9.2939e−06	1.2277e−05	9.0080e−06	3.5103e−06	7.2009e−07	1.0027e−06
R^2												
MFO	0.99994	1	1	1	0.99999	0.99999	0.99998	0.99848	0.99998	0.99960	1	0.99999
DEIM	0.99993	0.99993	1	0.99950	0.99960	1	0.99987	1	0.99986	0.99993	1	1
FPA	0.99984	0.99994	0.99986	0.99948	0.99961	0.99945	0.99970	0.99909	0.99987	0.99987	0.99924	0.99945

After the initialization, the P function is iteratively run until the T termination function is satisfied. The P function is the main function that moves the moths around the search space. As mentioned before, the inspiration of this algorithm is the transverse orientation of moths. Thus, the logarithmic spiral function is chosen as the main updated mechanism of the position of each moth with respect to the flame [32].

The position of each moth with respect to a flame is updated as follows Eq. (13):

$$M_i = S(M_i, F_j) \tag{13}$$

The logarithmic spiral for the MFO algorithm is Eq. (14):

$$S(M_i, F_j) = D_i \cdot e^{bt} \cdot \cos(2\pi t) + F_j \tag{14}$$

where M_i indicate the i-th moth, F_j indicates the j-th flame, and S is the spiral function. D_i indicates the distance of the i-th moth for the j-th flame, b is a constant for defining the shape of the logarithmic spiral, and t is a random number in $[r, 1]$. Adaptive convergence constant r linearly decreases from -1 to -2 to accelerate convergence around the flames over the course of iterations. The lower the t, the closer the distance to the flame [32].

D is calculated as follows Eq. (15):

$$D_i = |F_j - M_i| \tag{15}$$

The spiral equation allows a moth to fly around a flame and not necessarily in the space between them. Fig. 5 illustrates the updated moth positions around the flame. Exploration occurs when the next position outsides the space between the moth and the flame as can be illustrated in the arrows labeled 1, 3, and 4. Exploitation happens when the next position lies inside the space between the moth and flame as observed in the arrow labeled 2. To balance between the exploration and exploitation, the number of flames adaptively decreases over the iterations as in Eq. (16). Consequently, the moths update their positions only with respect to the best flame in the final steps of iterations.

$$flame\ no = round\left(N - l \times \frac{N-1}{T}\right) \tag{16}$$

where l is the current number of iteration, N is the maximum number of flames, and T is the maximum number of iterations. The flowchart of the MFO technique is displayed in the following Fig. 6:

There are some interesting observations for the MFO algorithm are presented in the following points:

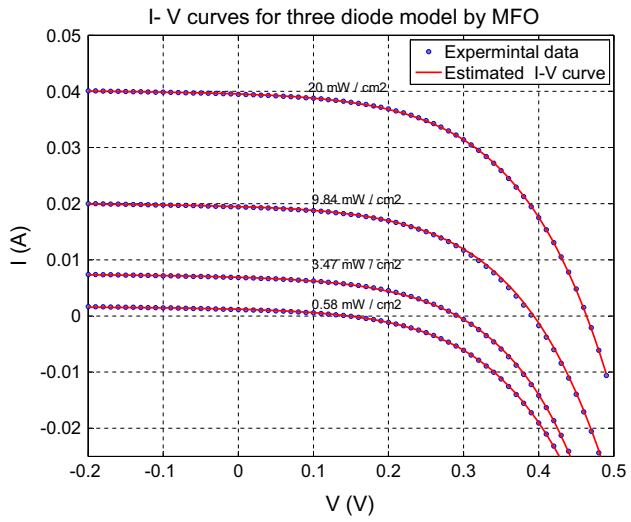

Fig. 9. Comparison between the experimental and the estimated (I-V) characteristic curves for TDM of Q6-1380 solar cell using MFO algorithm at different irradiance and room temperature.

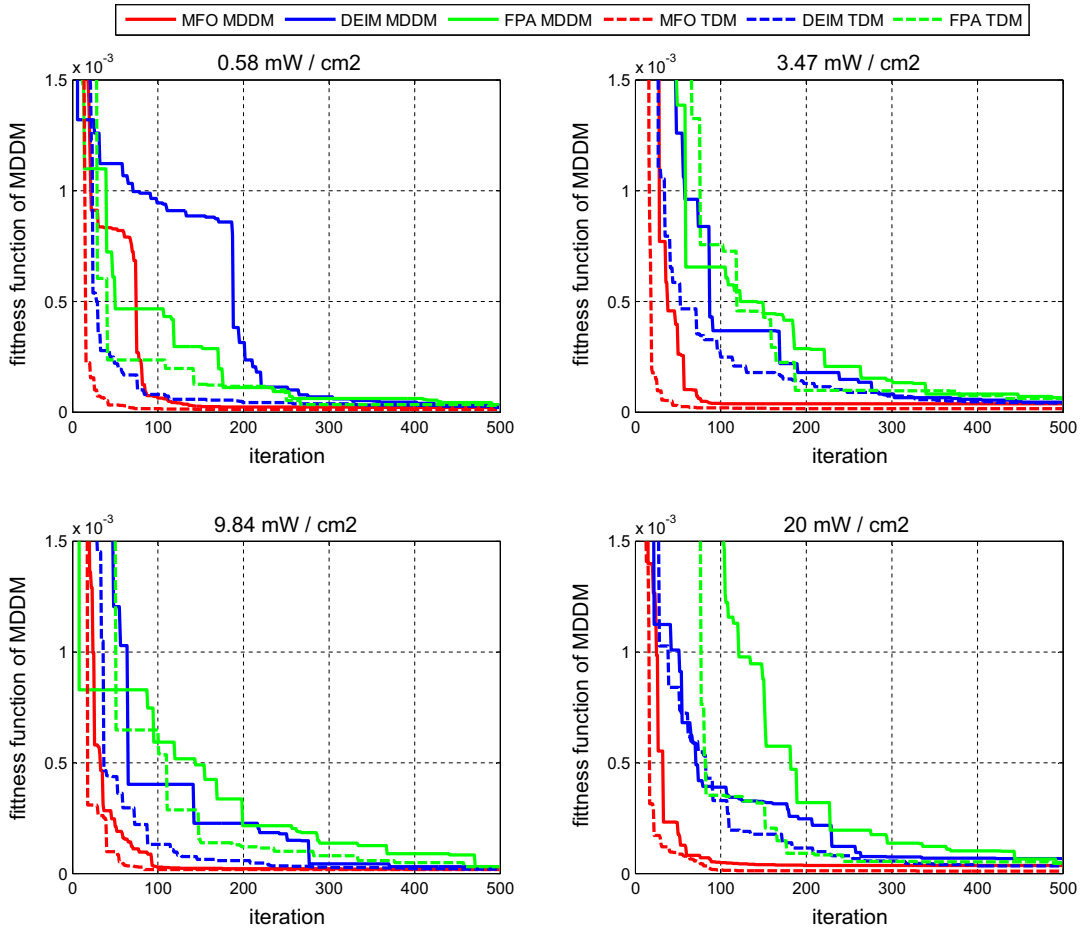

Fig. 10. The fitness function with respect to iteration numbers of MFO algorithm for MDDM and TDM of Q6-1380 solar cell.

- Assigning each moth a flame and updating the sequence of flames in each iteration increase exploration of the search space and decreases the probability of local optima stagnation.
- Considering the recent best solution obtained so far as the flames saves the promising solutions as the guides for moths. Consequently, the moths never get lost and the convergence of the MFO algorithm will be guaranteed.
- Adaptive number of flames balances exploration and exploitation.
- Adaptive convergence constant (r) causes accelerated convergence around the flames over the course of iterations.

The main requirements to apply the MFO, DEIM and FPA algorithms for the parameters estimation problem are reported as follows:

After a number of runs have been performed, the maximum number of iterations was chosen to be $T = 500$. The population size N was chosen equal to 70, because the population size N ranges between $[5d\ 10d]$ and in this work, $d = 7$ for DDM as well as TDM, while MDDM has 8 unknown parameters.

The mutation control factor F and the crossover rate CR in DEIM technique are automatically adjusted, parameter ϵ_1 is set to 0.28 and the DE/best/1/bin strategy is utilized [22].

The probability switch P in FPA algorithm is set to 0.8 [1].

5. Evaluation analysis

To ensure that the proposed algorithm has the ability to extract the unknown parameters accurately, a deeper analysis such as the MBE, AE and the Coefficient of Determination (R^2) is carried out.

The MBE is a statistical quantity which measures the performance of the model.

$$\mathrm{MBE} = \frac{1}{K}\sum_{i=1}^{K}(I_e - I_{exp}) \tag{17}$$

where k is the number of the readings of the measured data and I_e, I_{exp} are the estimated and the experimental currents respectively.

The AE can be defined as the absolute difference between I_e and I_{exp} currents under the same conditions of irradiance and temperature.

$$\mathrm{AE} = |I_e - I_{exp}| \tag{18}$$

The R^2 is used as a guideline to measure the accuracy of the model. R^2 has an values between 0 and 1. When R^2 equal 1, this means the consistency between the simulation and experimental results.

Table 3
Execution time consumed by MFO algorithm for the three models of Q6-1380 solar cell.

Algorithm	Execution time		
	DDM	MDDM	TDM
MFO	4.0169	13.2630	4.9521
DEIM	32.9635	75.4331	34.0339
FPA	10.2007	25.7724	10.9264

$$R^2 = 1 - \frac{\sum_{i=1}^{K}(I_e - I_{exp})^2}{\sum_{i=1}^{K}(I_{exp} - \overline{I_{exp}})} \quad (19)$$

where $\overline{I_{exp}}$ is the arithmetic mean of experimental current is calculated by the following Eq. (20).

$$\overline{I_{exp}} = \frac{1}{K}\sum_{i=1}^{K} I_{exp} \quad (20)$$

Also, the execution time is determined to indicate the time which the algorithms consume until reaching the maximum number of iterations.

6. Simulations and results

In this section, the estimation of the parameters of the three suggested models is accomplished. Therefore, a new optimization algorithm that is named MFO algorithm is proposed to extract the models' parameters and its results are compared to the results of two recent algorithms, namely DEIM and FPA techniques, are developed from the previous work in the literature. The comparison is implemented under two cases studies. The first case study is based on a reported data in literature [12] for the 7.7 cm^2 partition of Q6-1380 multi-crystalline solar cell under different irradiance levels. The second one is based on a measured data at

Table 4
The extracted parameters for DDM. MDDM and TDM for CS6P-240P solar module by MFO and DEIM, FPA techniques at different levels of irradiance and temperature.

Irradiance levels		Parameters									
		R_S (Ω)	R_{S2} (Ω)	R_{SH} (Ω)	I_{O1} (μA)	a_1	I_{O2} (mA)	a_2	I_{O3} (mA)	a_3	I_{PV} (A)
At 109.2 W/m^2, 37.32 °C	*DDM*										
	MFO	0.2000	–	811.282	0.25520	1.3104	1.000e−3	4.7949	–	–	0.99364
	DEIM	0.2000	–	736.2486	0.2256	1.2998	6.7156e−3	3.6642	–	–	0.99398
	FPA	0.32073	–	4201.42	0.61984	1.3880	5.135e−3	3.3378	–	–	0.98799
	MDDM										
	MFO	0.1385	1.96078	3938.5097	0.47719	1.3666	1.00e−3	4.79981	–	–	0.9926
	DEIM	0.1114	1.8334	3464.7789	0.35769	1.3380	4.4566e−04	3.0208	–	–	0.99139
	FPA	0.2074	1.1583	2541.8000	0.56228	1.3791	1.235e−03	3.1666	–	–	0.99070
	TDM										
	MFO	0.7337	–	450.1573	2.2787e−3	–	1.0692e−06	–	9.9999e−04	3.71730	0.99853
	DEIM	0.7351	–	449.3420	2.2658e−3	–	3.1652e−05	–	4.9986e−04	3.3526	0.9985
	FPA	0.7230	–	473.4507	2.2761e−3	–	1.0399e−04	–	5.9827e−04	3.7569	0.9978
At 246.65 W/m^2, 40.05 °C	*DDM*										
	MFO	0.200	–	4950.021	0.30245	1.2825	1.001e−3	4.8796	–	–	2.1427
	DEIM	0.200	–	49995.560	0.23539	1.2616	1.2423e−3	3.2728	–	–	2.1503
	FPA	0.2016	–	958.1916	0.37756	1.3021	8.9667e−3	3.7341	–	–	2.1502
	MDDM										
	MFO	0.25436	1.95231	3696.2415	0.1376	1.2216	9.859e−3	4.8999	–	–	2.1413
	DEIM	0.12289	1.7302	3299.2157	0.58340	1.3387	5.923e−4	3.7277	–	–	2.1427
	FPA	0.26256	1.1289	2050.7105	0.04418	1.14264	5.2881e−4	3.8824	–	–	2.15474
	TDM										
	MFO	0.45333	–	4989.2552	3.3585e−03	–	1.620e−03	–	0.9391	3.5252	2.1435
	DEIM	0.8932	–	4746.0897	3.4402e−3	–	9.9684e−04	–	1.025e−03	3.5697	2.1498
	FPA	0.4923	–	4889.4382	3.4530e−03	–	5.4342e−04	–	9.0503e−04	3.6523	2.1484
At 347.8 W/m^2, 43.95 °C	*DDM*										
	MFO	0.2532	–	2528.635	0.22983	1.2248	1.006e−3	4.8878	–	–	3.0315
	DEIM	0.2579	–	4685.515	0.32439	1.2514	2.8671e−4	3.35762	–	–	3.0328
	FPA	0.20032	–	550.214	0.32308	1.2517	1.005e−3	4.0037	–	–	3.0424
	MDDM										
	MFO	0.19048	1.8925	3520	0.61286	1.30251	9.9894e−03	4.9513	–	–	3.03145
	DEIM	0.22154	1.56071	2910.07250	0.32295	1.2505	3.0647e−4	3.0523	–	–	3.03814
	FPA	0.15366	1.1187	2865.7354	0.80036	1.3258	9.3395e−4	4.3508	–	–	3.03873
	TDM										
	MFO	0.41630	–	461.524	5.6724e−03	–	9.9850e−04	–	1.0234e−03	3.2256	3.0457
	DEIM	0.41479	–	465.3848	5.6773e−3	–	9.9482e−03	–	1.3562e−03	3.6897	3.0454
	FPA	0.42925	–	517.4005	5.6211e−03	–	5.3506e−04	–	9.6777e−4	3.1541	3.04277
At 580.3 W/m^2, 51.91 °C	*DDM*										
	MFO	0.2998	–	4998.5689	0.51487	1.2078	0.2941	4.89558	–	–	5.9592
	DEIM	0.2981	–	3335.5831	0.49873	1.2055	3.892e−3	4.03551	–	–	5.9511
	FPA	0.3068	–	3677.6104	0.47645	1.2028	4.521e−3	3.6326	–	–	5.9336
	MDDM										
	MFO	0.2927	1.8574	3825.0038	0.63357	1.2234	1.523e−02	4.98952	–	–	5.95992
	DEIM	0.31652	1.4772	3693.4323	0.36225	1.18424	4.4165e−4	4.1983	–	–	5.9102
	FPA	0.3185	1.10681	2473.952	0.28395	1.1656	3.9795e−4	4.0584	–	–	5.9556
	TDM										
	MFO	0.38481	–	461.8669	1.7346e−02	–	9.210e−04	–	1.210e−03	3.2135	6.00066
	DEIM	0.38524	–	457.282	1.73635e−2	–	9.9751e−04	–	1.0234e−03	3.2658	6.0016
	FPA	0.39137	–	457.0546	1.7297e−02	–	8.7857e−04	–	9.0089e−04	3.2926	6.00755

laboratory for CS6P-240P multi-crystalline solar module under different environmental conditions.

6.1. Case study 1

In this case, multi-crystalline solar cell Q6-1380 is taken as a sample to be investigated. The dimension of the cell under test is 7.7 $(cm)^2$, the (I-V) characteristic curves of this cell is obtained from the previous literature [12]. Four different levels of irradiance such as 20, 9.84, 3.47, and 0.58 mW/cm^2 at room temperature are studied. The length of the experimental (I-V) data points for various environmental conditions is equal. DDM, MDDM and TDM models are introduced to emulate this cell. MFO, DEIM and FPA algorithms are applied on the three models to extract their unknown parameters.

The MFO, DEIM and FPA algorithms are executed to extract the unknown parameters of the three models. The estimated parameters are listed in Table 1 and the RMSE values are plotted in Fig. 7. It's observed from Fig. 7 that the first rank in reduction of the calculated RMSE is achieved by using the extracted parameters of the TDM followed by that of the MDDM, while the last rank is obtained by the DDM at all levels of irradiance under test. Moreover, it can be noticed that for each model the least value of the RMSE is achieved by MFO algorithm followed by DEIM then FPA techniques.

Furthermore, the AE curves of the detailed models such as MDDM and TDM are plotted to verify the accuracy of the estimated parameters. Fig. 8 shows that the MFO technique exhibits less absolute errors compared with the other algorithms specially when accomplished with TDM. While the results of DEIM and FPA techniques are relatively closed to each other.

For more justification, a detailed evaluation analysis is established to calculate the RMSE, MBE, AE at MPP and R^2 which are reported in Table 2. The mean values of the computed RMSE of the TDM are equal to $7.33e-5$, $1.1475e-4$ and $1.65e-4$ for MFO, DEIM and FPA algorithms respectively. While the mean values of the calculated MBE are equal to $1.1439e-7$, $1.821e-6$ and $4.46e-5$ for MFO, DEIM and FPA algorithms respectively. Additionally, the mean values of AE at MPP are equal to $2.5855e-5$, $3.047e-5$ and $1.9155e-5$ for MFO, DEIM and FPA algorithms respectively. The previous results prove that the MFO in conjunction with TDM has the best accuracy. Thus, the (I-V) characteristic curves of the extracted parameters of TDM that are obtained by MFO and the experimental data are plotted in Fig. 9, this figure illustrates that the extracted parameters achieve the least variation between the two curves.

In addition, the most essential factors of the comparison process between MFO algorithm and the other techniques are the speed of conversion and the execution time until reaching the maximum number of iterations. Fig. 10 illustrates that MFO algorithm converges to the optimal solution faster than the DEIM and FPA techniques for both of MDDM and TDM models. The execution time of MFO is a bout 50% of that of FPA, while it is about 15% of that of

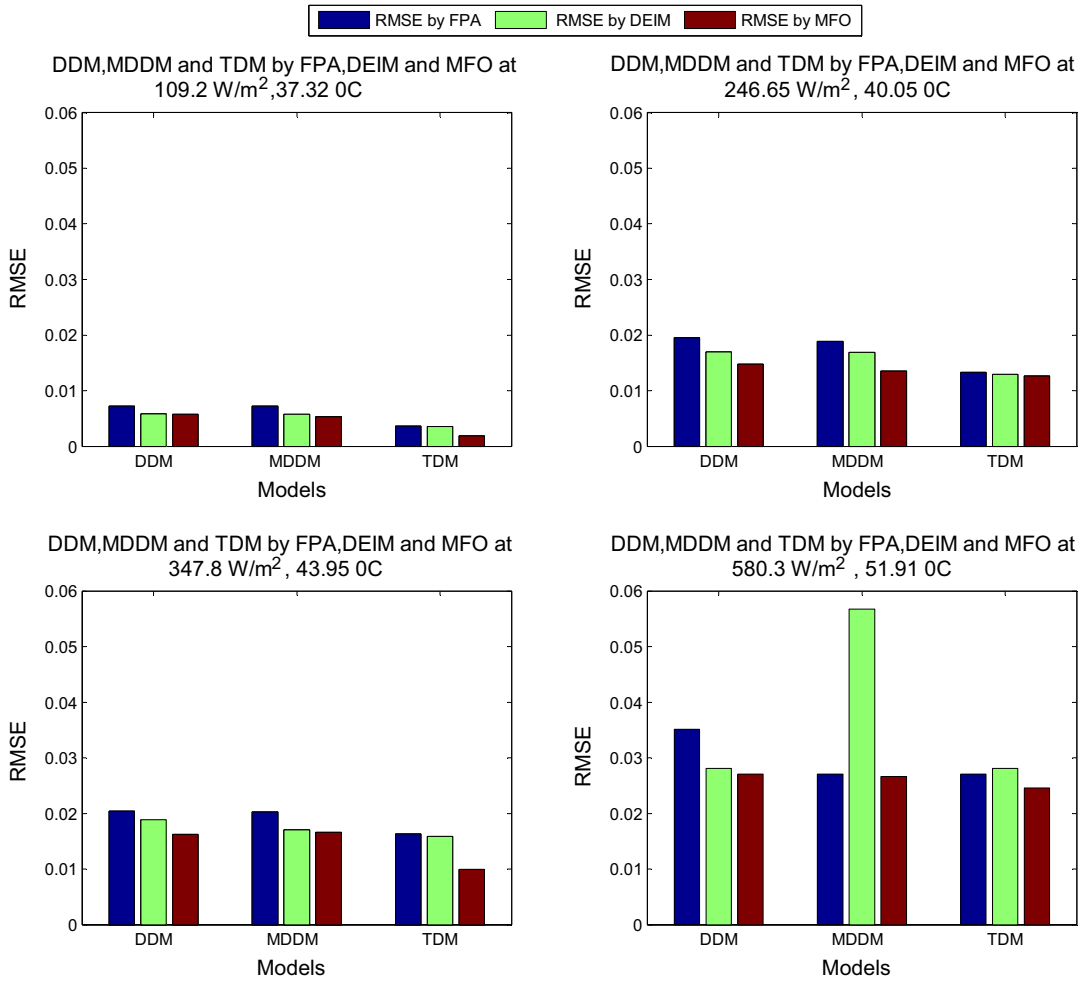

Fig. 11. RMSE for DDM, MDDM and TDM models of CS6P-240P solar module by FPA, DEIM and MFO algorithms at different environmental conditions.

DEIM as listed in Table 3 for all the three models and at all the entire ranges of irradiance and room temperature. Consequently, it should be noticed that, the MFO algorithm converges to the optimal solution more rapidly and more accurately compared with the DEIM and FPA algorithms. That's because the nature of the inspiration of MFO algorithm which helps it to never lose its optimal solutions and converges to the solution rapidly.

The final results after applying MFO, DEIM and FPA algorithms on the three selected models (DDM, MDDM and TDM) for multi-crystalline solar cell are that the TDM has the best performance when accomplished by MFO algorithm in terms of the physical behavior, error analysis, speed of conversion, execution time and the (I-V) curves justification.

6.2. Case study 2

In this case, the modeling for multi-crystalline PV solar module CS6P-240P is established based on experimental data measured at the laboratory. The (I-V) data is measured at four levels of irradiance and temperature which are (673.5, 580.3, 347.8, 246.65, and 109.2 W/m^2) with(45.92, 51.91, 43.95, 40.05, and 37.32 °C) respectively. The measuring instruments are as follows: (I-V) 400 PHOTOVOLTAIC PANEL ANALYZER with HT304N radiating sensor and temperature sensor PT300. The TOPVIEW software is used to add this data to personal PC.

The unknown parameters of the DDM, MDDM and TDM are estimated by using the three proposed algorithms and are tabulated in Table 4. Depending on the extracted parameters, the RMSE is computed for the three suggested models and it's values are plotted in Fig. 11. Fig. 11 shows that the least value of RMSE is achieved by using the estimated parameters of the TDM followed by that of the MDDM and then that of the DDM over the entire ranges of the environmental conditions under test. Also, it can be observed that for each model the least value of the RMSE is achieved by MFO algorithm while the RMSE values of DEIM and FPA algorithms are fluctuated over the four environmental conditions under test.

In addition, AE curves are drawn for MDDM and TDM, to validate the accuracy of the extracted parameters by the proposed algorithm. Fig. 12 illustrates that the MFO algorithm has the lowest AE curves, while the DEIM and FPA algorithms exchange their rules at the four cases of the weather conditions under test.

Additionally, a more detailed comparison among the proposed algorithm, DEIM and FPA techniques is performed in Table 5. Table 5 presents that the highest value for R^2 and the least values of RMSE, MBA and AE at MPP are obtained by applying MFO on TDM. The previous mentioned results indicate that the MFO algorithm accomplished with TDM achieves the most accurate model for the multi-crystalline solar module. Consequently, the (I-V) curves of the estimated parameters of TDM that are obtained by MFO and the experimental data are drawn in Fig. 13. Fig. 13 shows that the best fitting between the two curves.

Furthermore, the most important aspects of the comparison process between MFO algorithm and the DEIM and FPA methods are the speed of conversion and the execution time. Fig. 14 illustrates that MFO algorithm converges to the optimal solution rapidly compared with the other algorithms. Table 6 indicates that the execution time of DEIM technique is seven times of that of MFO algorithm, while the execution time of FPA method is double that of the MFO technique.

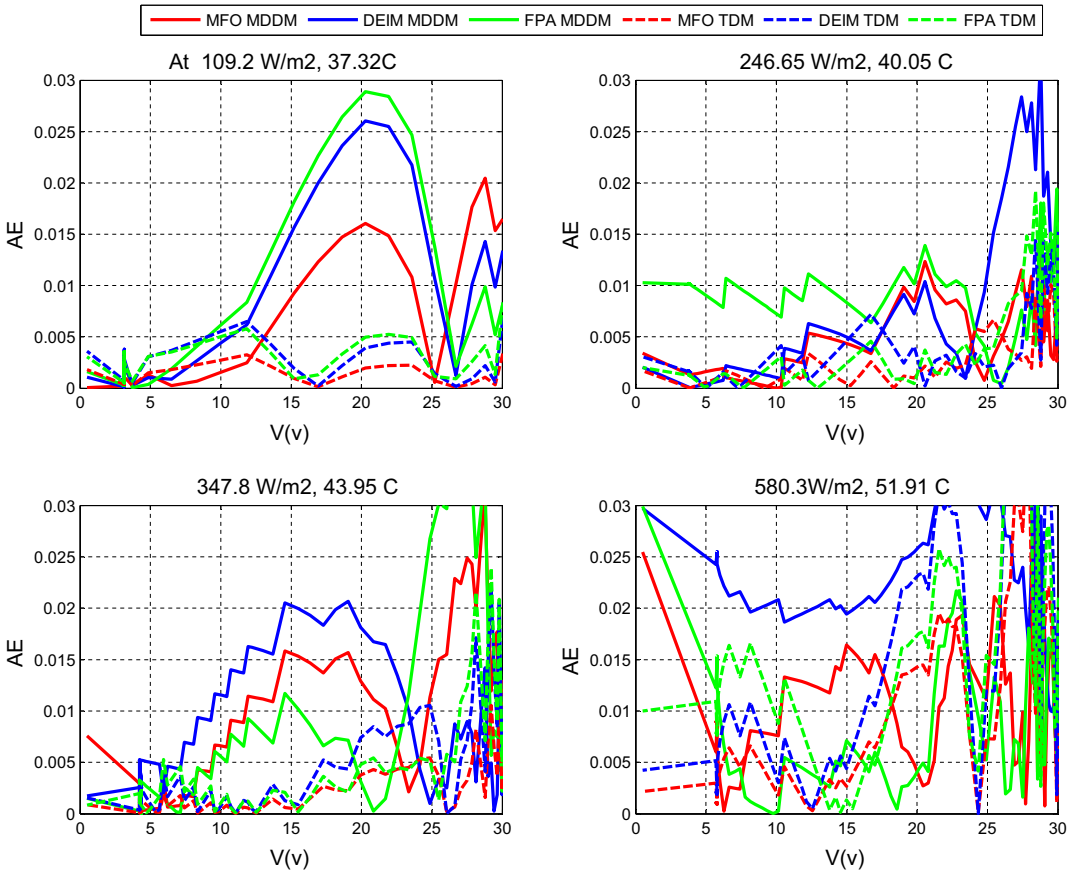

Fig. 12. Absolute error with respect to module voltage for MDDM and TDM by different algorithms at different environmental conditions.

Table 5
RMSE, MBE, AE at MPP and R^2 of various techniques for three models of the solar module under different environmental conditions.

	At 109.2 W/m^2, 37.32 °C			At 246.65 W/m^2, 40.05 °C			At 347.8 W/m^2, 43.95 °C			At 580.3 W/m^2, 51.91 °C		
	DDM	MDDM	TDM	DDM	MDDM	TDM	DDM	MDDM	TDM	DDM	MDDM	TDM
RMSE												
MFO	0.005720	0.005326	0.00185507	0.01479	0.013537	0.0126026	0.01626	0.016583	0.009927	0.02705	0.026664	0.02455
DEIM	0.005798	0.005721	0.0035508	0.01693	0.01685	0.012913	0.01885	0.0170534	0.015864	0.02813	0.056742	0.02807
FPA	0.007229	0.007205	0.0036073	0.01950	0.01886	0.013287	0.02042	0.020247	0.016307	0.03511	0.02709	0.02708
MBE												
MFO	2.269e−6	2.217e−06	8.604e−07	2.218e−5	7.636e−06	9.182e−07	9.116e−06	1.187e−05	5.009e−07	6.839e−06	1.781e−06	1.457e−06
DEIM	6.309e−4	1.407e−04	7.7809e−06	5.548e−03	1.376e−03	2.2471e−05	3.780e−04	6.4088e−03	1.874e−05	6.145e−03	7.849e−03	6.974e−05
FPA	2.125e−3	7.559e−04	2.929e−04	3.328e−03	1.0593e−03	9.3349e−04	1.836e−04	3.038e−03	1.581e−04	1.757e−03	1.283e−03	1.1523e−03
AE at MPP												
MFO	0.0102	0.00100	8.9771e−05	0.0163	0.0093	0.0023	0.0574	0.0229	0.0203	0.0893	0.0506	0.0304
DEIM	0.0122	0.0012	1.7935e−04	0.051	0.0255	0.0028	0.0505	0.0479	0.0401	0.0954	0.0597	0.0481
FPA	0.0282	0.0021	9.0362e−04	0.0377	0.0050	0.0049	0.0798	0.0795	0.0345	0.1150	0.0836	0.0473
R^2												
MFO	0.99945	0.99955	0.99979	0.99962	0.99968	0.99972	0.99975	0.99971	0.99978	0.99983	0.99983	0.99987
DEIM	0.99945	0.99952	0.99979	0.99953	0.99958	0.99971	0.99969	0.99968	0.99978	0.99982	0.99928	0.99982
FPA	0.99802	0.99907	0.99978	0.99934	0.99938	0.99969	0.99963	0.99961	0.99976	0.99972	0.99983	0.99983

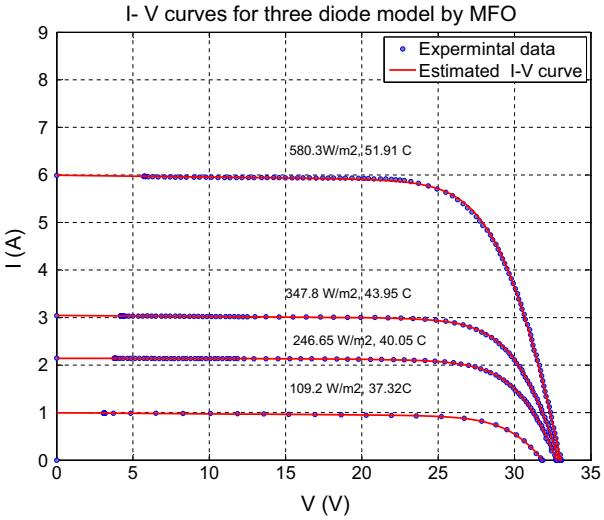

Fig. 13. Comparison between the experimental and the estimated (I-V) characteristic curves for TDM of CS6P-240P using MFO algorithm under different environmental conditions.

The main findings after applying MFO, DEIM and FPA algorithms on the three selected models (DDM, MDDM and TDM) for multi-crystalline solar module show that the three diode model has the best performance when accomplished by the MFO algorithm from the point of view of the physical behavior, error analysis, speed of conversion, execution time and the (I-V) curves justification.

7. Conclusion

The multi-crystalline solar cells/modules are widely used elements in the PV systems commercially. To increase the efficiency of the PV system design, an accurate modeling should be provided. Therefore, more detailed models such as modified double diode and three diode models are investigated to account for the physical complexity of the multi-crystalline cell/module such as effect of the grain boundaries, the carrier recombination and the leakage current, as well as a double diode model as a generic model. Moth-Flame Optimization Algorithm is proposed as a new optimization technique to extract the three models' parameters. Similarly, another two previously published optimization algorithms namely Hybrid Evolutionary, FLower Pollination Algorithm are also applied on theses models.

It's observed from the results of the three applied algorithms on the three suggested models that the MFO algorithm shows the best performance upon it's application on TDM in terms of the most accurate representation of the physical behavior for the multi-crystalline solar cells/modules, the least RMSE, MBE and AE at MPP, the best (I-V) curve fitting, the fastest convergence speed and the shortest execution time for the DEIM and FPA algorithms. Additionally, MFO algorithm was found to be superior compared to DEIM and FPA algorithms in its nature of the inspiration that helps it to never lose its optimal solutions and converges to the solution rapidly. Therefore, the MFO technique accomplished with TDM model are recommend in this investigation. Consequently, the accurate model of the multi-crystalline solar cells/modules is fulfilled which reflected on the accuracy of the performance of the whole solar system design.

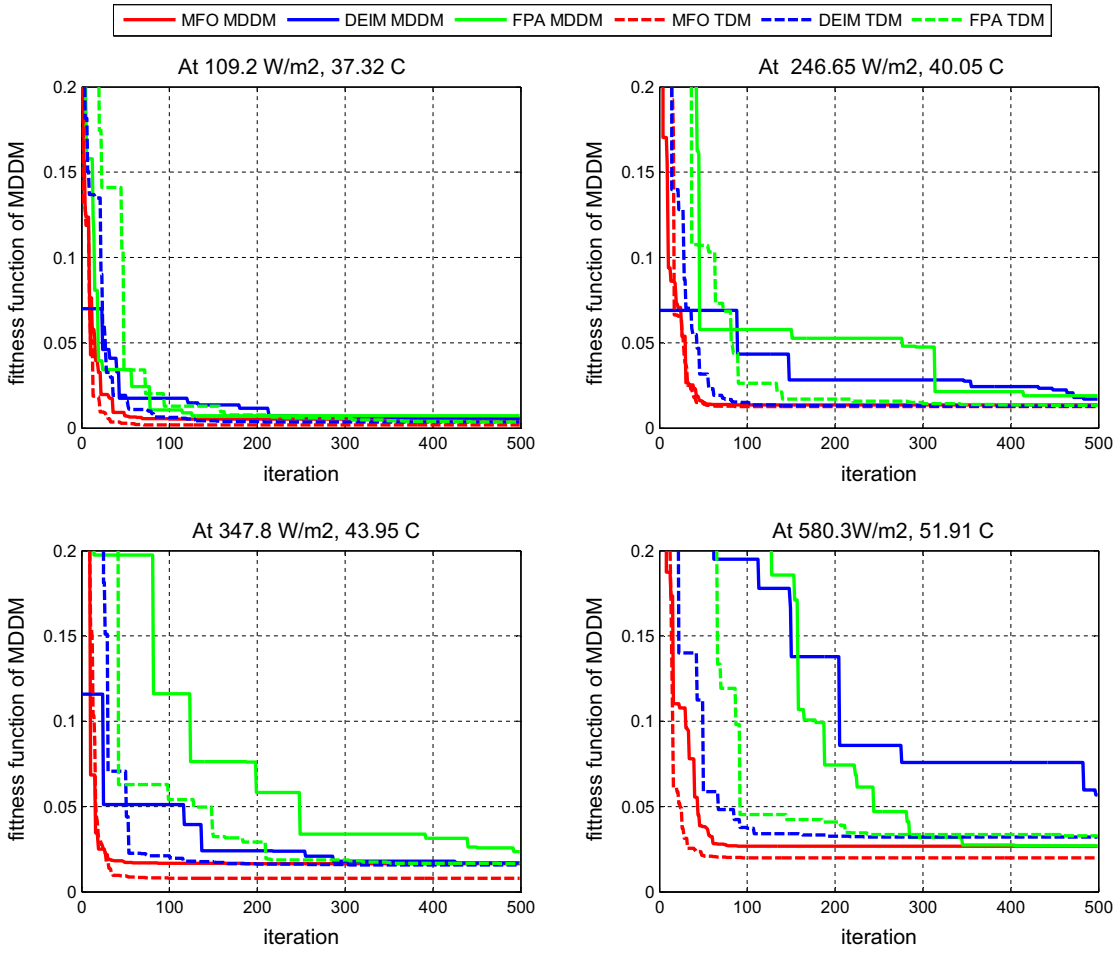

Fig. 14. The values of fitness function with respect to iteration numbers of MFO algorithm for MDDM and TDM of CS6P-240P solar module.

Table 6
Execution time consumed by MFO algorithm for the three models of CS6P-240P solar module.

Algorithm	Execution time		
	DDM	MDDM	TDM
MFO	4.068678	13.285164	5.052748
DEIM	33.23153	79.35685	35.15398
FPA	9.647589	25.02548	10.776520

References

[1] Alam D, Yousri D, Eteiba M. Flower pollination algorithm based solar PV parameter estimation. Energy Convers Manage 2015;101:410–22.
[2] Tang X, Francis LA, Gong L, Wang F, Raskin J-P, Flandre D, et al. Characterization of high-efficiency multi-crystalline silicon in industrial production. Sol Energy Mater Sol Cells 2013;117:225–30.
[3] Gu X, Yu X, Guo K, Chen L, Wang D, Yang D. Seed-assisted cast quasi-single crystalline silicon for photovoltaic application: towards high efficiency and low cost silicon solar cells. Sol Energy Mater Sol Cells 2012;101:95–101.
[4] Derbali L, Ezzaouia H. Efficiency improvement of multicrystalline silicon solar cells after surface and grain boundaries passivation using vanadium oxide. Mater Sci Eng: B 2012;177(13):1003–8.
[5] Derbali L, Ezzaouia H. Electrical properties improvement of multicrystalline silicon solar cells using a combination of porous silicon and vanadium oxide treatment. Appl Surf Sci 2013;271:234–9.
[6] Mukherjee S, Farid S, Stroscio MA, Dutta M. Modeling polycrystalline effects on the device characteristics of cdte based solar cells. In: 2015 International workshop on computational electronics (IWCE). IEEE; 2015. p. 1–4.
[7] Ghosh AK, Fishman C, Feng T. Theory of the electrical and photovoltaic properties of polycrystalline silicon. J Appl Phys 1980;51(1):446–54.
[8] Lee S, Lim D, Yi J. Novel type of multicrystalline silicon solar cell with an additional electrode along the grain boundaries. J-Kor Phys Soc 2000;37 (1):64–8.
[9] Joshi D, Sharma K. Effects of grain boundaries on the performance of polycrystalline silicon solar cells. Indian J Pure Appl Phys 2012;50(9):661–9.
[10] Kurobe K-I, Matsunami H. New two-diode model for detailed analysis of multicrystalline silicon solar cells. Jpn J Appl Phys 2005;44(12R):8314.
[11] Nishioka K, Sakitani N, Uraoka Y, Fuyuki T. Analysis of multicrystalline silicon solar cells by modified 3-diode equivalent circuit model taking leakage current through periphery into consideration. Sol Energy Mater Sol Cells 2007;91 (13):1222–7.
[12] Kassis A, Saad M. Analysis of multi-crystalline silicon solar cells at low illumination levels using a modified two-diode model. Sol Energy Mater Sol Cells 2010;94(12):2108–12.
[13] Chin VJ, Salam Z, Ishaque K. Cell modelling and model parameters estimation techniques for photovoltaic simulator application: a review. Appl Energy 2015;154:500–19.
[14] Brano VL, Ciulla G. An efficient analytical approach for obtaining a five parameters model of photovoltaic modules using only reference data. Appl Energy 2013;111:894–903.
[15] D.S. Chan, J.C. Phang, Analytical methods for the extraction of solar-cell single- and double-diode model parameters from IV characteristics.
[16] Ishaque K, Salam Z, Taheri H, et al. Modeling and simulation of photovoltaic (PV) system during partial shading based on a two-diode model. Simul Model Pract Theory 2011;19(7):1613–26.
[17] Elbaset AA, Ali H, Abd-El Sattar M. Novel seven-parameter model for photovoltaic modules. Sol Energy Mater Sol Cells 2014;130:442–55.
[18] Ishaque K, Salam Z, Mekhilef S, Shamsudin A. Parameter extraction of solar photovoltaic modules using penalty-based differential evolution. Appl Energy 2012;99:297–308.
[19] Awadallah MA. Variations of the bacterial foraging algorithm for the extraction of PV module parameters from nameplate data. Energy Convers Manage 2016;113:312–20.
[20] Chen X, Yu K, Du W, Zhao W, Liu G. Parameters identification of solar cell models using generalized oppositional teaching learning based optimization. Energy 2016;99:170–80.
[21] Muhsen DH, Ghazali AB, Khatib T, Abed IA. Extraction of photovoltaic module models parameters using an improved hybrid differential evolution/electromagnetism-like algorithm. Sol Energy 2015;119:286–97.

[22] Muhsen DH, Ghazali AB, Khatib T, Abed IA. Parameters extraction of double diode photovoltaic modules model based on hybrid evolutionary algorithm. Energy Convers Manage 2015;105:552–61.
[23] Yuan X, Xiang Y, He Y. Parameter extraction of solar cell models using mutative-scale parallel chaos optimization algorithm. Sol Energy 2014;108:238–51.
[24] Oliva D, Cuevas E, Pajares G. Parameter identification of solar cells using artificial bee colony optimization. Energy 2014;72:93–102.
[25] Askarzadeh A, Rezazadeh A. Artificial bee swarm optimization algorithm for parameters identification of solar cell models. Appl Energy 2013;102:943–9.
[26] Askarzadeh A, Rezazadeh A. Parameter identification for solar cell models using harmony search-based algorithms. Sol Energy 2012;86(11):3241–9.
[27] El-Naggar K, AlRashidi M, AlHajri M, Al-Othman A. Simulated annealing algorithm for photovoltaic parameters identification. Sol Energy 2012;86(1):266–74.
[28] AlRashidi M, AlHajri M, El-Naggar K, Al-Othman A. A new estimation approach for determining the I–V characteristics of solar cells. Sol Energy 2011;85(7):1543–50.
[29] Easwarakhanthan T, Bottin J, Bouhouch I, Boutrit C. Nonlinear minimization algorithm for determining the solar cell parameters with microcomputers. Int J Sol Energy 1986;4(1):1–12.
[30] Ismail M, Moghavvemi M, Mahlia T. Characterization of PV panel and global optimization of its model parameters using genetic algorithm. Energy Convers Manage 2013;73:10–25.
[31] Askarzadeh A, dos Santos Coelho L. Determination of photovoltaic modules parameters at different operating conditions using a novel bird mating optimizer approach. Energy Convers Manage 2015;89:608–14.
[32] Mirjalili S. Moth-flame optimization algorithm: a novel nature-inspired heuristic paradigm. Knowl-Based Syst 2015;89:228–49.
[33] Khanna V, Das B, Bisht D, Singh P, et al. A three diode model for industrial solar cells and estimation of solar cell parameters using PSO algorithm. Renew Energy 2015;78:105–13.
[34] Sah C-T, Noyce R, Shockley W. Carrier generation and recombination in pn junctions and pn junction characteristics. Proc IRE 1957;45(9):1228–43.
[35] Fossum JG, Lindholm FA. Theory of grain-boundary and intragrain recombination currents in polysilicon pn-junction solar cells. IEEE Trans Electr Dev 1980;27(4):692–700.
[36] Koohi-Kamal S, Rahim N, Mokhlis H, Tyagi V. Photovoltaic electricity generator dynamic modeling methods for smart grid applications: a review. Renew Sustain Energy Rev 2016;57:131–72.